

Altered plant carbon partitioning enhanced forest ecosystem carbon storage after 25 years of nitrogen additions

Brooke A. Eastman¹ , Mary B. Adams², Edward R. Brzostek¹ , Mark B. Burnham³ , Joseph E. Carrara¹ , Charlene Kelly⁴ , Brenden E. McNeil⁵ , Christopher A. Walter¹  and William T. Peterjohn¹

¹Department of Biology, West Virginia University, Life Sciences Building, 53 Campus Drive, Morgantown WV 26506, USA; ²USDA Forest Service, 180 Canfield Street, Morgantown WV 26506, USA; ³Center for Advanced Bioenergy and Bioproducts Innovation, University of Illinois Urbana-Champaign, 1200 IGB, 1206 West Gregory Drive, Urbana IL 61801, USA; ⁴Division of Forestry and Natural Resources, West Virginia University, 337 Percival Hall, Morgantown WV 26506, USA; ⁵Department of Geology and Geography, West Virginia University, Brooks Hall, 98 Beechurst Ave., Morgantown WV 26506, USA

Summary

Author for correspondence:
Brooke A. Eastman
Email: be0011@mix.wvu.edu

Received: 16 October 2020
Accepted: 29 January 2021

New Phytologist (2021)
doi: 10.1111/nph.17256

Key words: carbon cycling, experimental N addition, N acquisition strategies, optimal allocation theory, plant biomass allocation, temperate forest, terrestrial carbon sink.

- Decades of atmospheric nitrogen (N) deposition in the northeastern USA have enhanced this globally important forest carbon (C) sink by relieving N limitation. While many N fertilization experiments found increased forest C storage, the mechanisms driving this response at the ecosystem scale remain uncertain.
- Following the optimal allocation theory, augmented N availability may reduce belowground C investment by trees to roots and soil symbionts. To test this prediction and its implications on soil biogeochemistry, we constructed C and N budgets for a long-term, whole-watershed N fertilization study at the Fernow Experimental Forest, WV, USA.
- Nitrogen fertilization increased C storage by shifting C partitioning away from belowground components and towards aboveground woody biomass production. Fertilization also reduced the C cost of N acquisition, allowing for greater C sequestration in vegetation. Despite equal fine litter inputs, the C and N stocks and C : N ratio of the upper mineral soil were greater in the fertilized watershed, likely due to reduced decomposition of plant litter.
- By combining aboveground and belowground data at the watershed scale, this study demonstrates how plant C allocation responses to N additions may result in greater C storage in both vegetation and soil.

Introduction

Historically high rates of nitrogen (N) deposition across temperate forests in the Northern Hemisphere (Galloway *et al.*, 2008; Fowler *et al.*, 2013) have often alleviated N-limitation (LeBauer & Treseder, 2008) and enhanced this important terrestrial carbon (C) sink (Pan *et al.*, 2011; Schulte-Uebbing & de Vries, 2017; O'Sullivan *et al.*, 2019). Experimental N additions to aggrading temperate forests typically cause greater biomass accumulation, decreased soil respiration, and enhanced soil C (Xia & Wan, 2008; Janssens *et al.*, 2010; Liu & Greaver, 2010; Lovett *et al.*, 2013; Frey *et al.*, 2014; de Vries *et al.*, 2014). However, few N addition experiments have persisted long enough at an ecologically relevant spatial scale to allow a more complete expression of mechanisms that enhance woody biomass or the feedback of plant responses to soil biogeochemistry. Plant–microbial interactions significantly shape the biogeochemistry of ecosystems through the exchange of C for N between plants and microbes, which modulates plant net primary productivity (NPP) and alters the stabilization and mineralization of soil C (Chapman *et al.*, 2006; Drake *et al.*, 2011; Phillips *et al.*, 2013; Terrer

et al., 2016). Thus, quantifying the responses of both above- and below-ground ecosystem components to experimental N additions is needed to determine the mechanisms underlying these responses, and to predict how these ecosystems will respond to reduced N inputs and other environmental changes (Schmidt *et al.*, 2011; Averill & Waring, 2017; Zak *et al.*, 2017).

Such widely observed responses to experimental N additions (e.g. enhanced aboveground biomass and reduced soil respiration) are generally consistent with the optimal allocation theory of Bloom *et al.* (1985), in which plants adjust to optimally partition resources for the acquisition of the most limiting resource. Given this theory, ‘subsidies’ of N to a N-limited ecosystem should reduce the C cost of N acquisition by lessening N limitation, allowing plants to partition C towards acquiring other limiting resources (e.g. light; Johnson *et al.*, 1997; Mohan *et al.*, 2014). Consequently, we expect elevated N inputs to shift plant C flux away from belowground N acquisition and towards aboveground productivity. Given recent research highlighting the importance of belowground C inputs in fueling decomposition (Sulman *et al.*, 2017), this allocation shift could initiate a plant–soil feedback in which less C flux to mycorrhizas and microbial

priming of soil organic matter (SOM) decomposition may increase soil C stocks (Gill & Finzi, 2016; Carrara *et al.*, 2018) and ultimately reduce mineralization rates of essential plant nutrients. An important assumption of optimal resource allocation theory is that resource availability changes slowly through synchronous changes in C and N fluxes, and it is uncertain whether the theory applies at the whole-ecosystem scale and in ecosystems experiencing fairly rapid changes in the environment – such as N additions (Bloom *et al.* 1985; Phillips *et al.* 2013).

Unsurprisingly, many gaps in our empirical knowledge of ecosystem responses to N deposition are mirrored in Earth system models (ESMs), at times leading to uncertain predictions of the future C sink. Recent model improvements have used observational benchmarks to improve the representation of C–N dynamics (Thornton *et al.*, 2007; Wieder *et al.*, 2015; Terrer *et al.*, 2019), and plant–microbe interactions (Shi *et al.*, 2016, 2019). Yet, these models do not capture the commonly observed reduction in soil respiration with N additions (Janssens *et al.*, 2010). Specifically, the current generation of ESMs often respond to elevated N deposition with increased NPP to all plant components and an accumulation of soil C through greater plant litter inputs, as opposed to a shift in C partitioning and subsequent decrease in

decomposition rates (Ise *et al.*, 2010; Bellassen *et al.*, 2011; Todd-Brown *et al.*, 2013; Fernández-Martínez *et al.*, 2014; Montané *et al.*, 2017; Sulman *et al.*, 2017). One reason models cannot capture these widespread ecosystem responses to N deposition is that their structures lack the plant–microbe interactions controlling these patterns (e.g. reduced belowground C flux slowing microbial decomposition; Fisher *et al.*, 2019; Meyerholt *et al.*, 2020). Thus, long-term experimental data are invaluable for clarifying mechanisms behind ecosystem responses and restructuring models to better capture the N impacts on global C cycling (Wieder *et al.*, 2019; Davies-Barnard *et al.*, 2020).

In this study, we utilized data from the whole-watershed N addition study at the Fernow Experimental Forest (Fernow) in West Virginia, USA, to examine the effects of > 25 yr of elevated N inputs on ecosystem C storage and partitioning. The abundant and long-term data from this site provide a rare opportunity to assess how N additions influence C and N interactions in a temperate deciduous forest over decadal time scales, and help clarify mechanisms that may influence the terrestrial C sink and constrain global C models. We constructed C and N budgets for two adjacent watersheds after > 25 yr of ammonium sulfate ((NH₄)₂SO₄) additions to one watershed. From these budgets, we synthesized the C and N stocks and fluxes of major forest ecosystem components, estimated changes in plant C allocation and identified some potential mechanisms behind the ecosystem response to chronic N additions. More specifically, we used these budgets to explore three questions: First, how do N additions affect tree C allocation and ultimately impact productivity over the long term? Second, does a reduction in the C cost of N acquisition act as an important mechanism driving changes in the plant C pools and fluxes with N additions? And third, what are the impacts of the tree responses to N addition on soil biogeochemistry?

Materials and Methods

Study site

Located in the Allegheny Mountain region of the Central Appalachian Mountains, the Fernow Experimental Forest, near Parsons, WV (39°1'48''N, 79°40'12''W), hosts over 80 yr of ecological monitoring and experimentation, including a whole-watershed N addition experiment (Adams *et al.*, 2012). Elevations range from 530–1115 m, and slopes are typically between 20 and 50%. Soils are shallow (< 1 m) and predominantly Calvin channery silt loam (Typic Dystrochrept), underlain with fractured sandstone and shale. Mean monthly air temperatures range from *c.* –2.8°C in January to *c.* 20°C in July, with a growing season from May through October (Table 1; Young *et al.*, 2019). Mean annual precipitation is *c.* 146 cm and is evenly distributed across seasons.

The whole-watershed N addition experiment consists of two adjacent watersheds in a broadleaf deciduous forest (Fig. 1). From January 1989 through October 2019, one watershed (+N WS3; 34 ha) received 3.5 g N m⁻² yr⁻¹ as (NH₄)₂SO₄, which was about double the rate of ambient N in throughfall at the start

Table 1 Site characteristics of a reference watershed (Ref WS7) and the adjacent N-fertilized watershed (+N WS3) in the Fernow Experimental Forest, WV, USA.

Characteristic	Ref WS7	+N WS3
Area (ha)	24	34
Aspect	East	South
Land use history	Upper 12 ha clearcut (1963); Maintained barren with herbicides (1964–1969); Lower 12 ha clearcut (1966); Entire watershed maintained barren with herbicide (1967–1969); Natural recovery (1969–present)	Intensive selection cut (1958–1959, 1963); patch cuttings totaling 2.3 ha (1968); clearcut except 3-ha shade strip along stream (1970); stream shade strip cut & natural recovery (1972); experimental N additions (1989–2019)
Annual precipitation (mm)	1460	1460
Mean air temperature (°C) ^a	9.3	9.3
Cumulative N deposition, 1989–2018 (g N m ⁻²)		
Experimental	0	104
Ambient ^b	26	26
Total	26	131
Soil pH ^c	4.52	4.12
Top four dominant species (by % basal area) ^d	<i>Liriodendron tulipifera</i> , <i>Betula lenta</i> , <i>Prunus serotina</i> , <i>Acer rubrum</i>	<i>P. serotina</i> , <i>A. rubrum</i> , <i>B. lenta</i> , <i>Quercus rubra</i>

^aFrom Young *et al.* (2019).

^bData from CASTNET total wet + dry N deposition.

^cMeans based on a 2011 soil sampling of 0–5 cm mineral soil at 100 points per watershed (Gilliam *et al.*, 2018).

^dData from 2016 to 2017 dendrometer plot census.

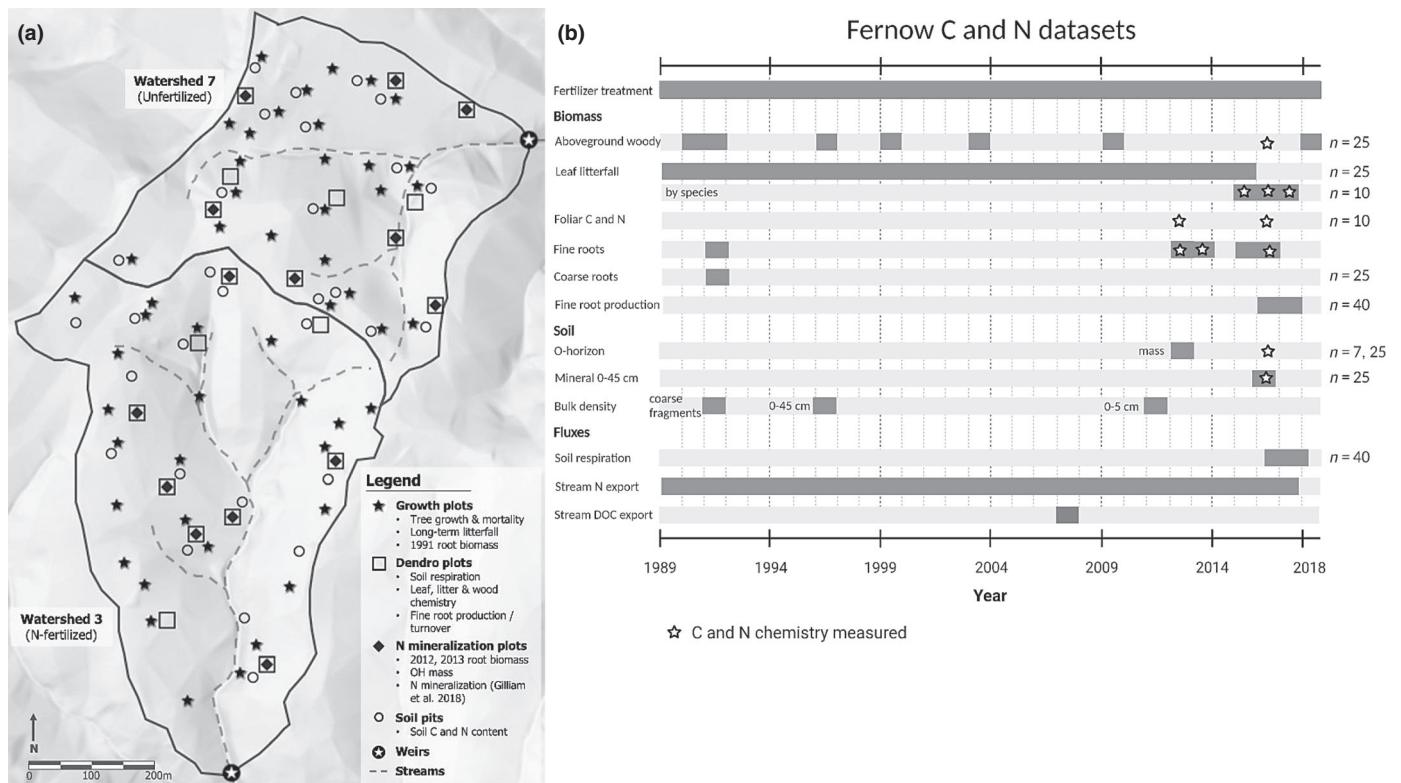


Fig. 1 (a) Map of the Fernow Experimental Forest and (b) data timeline of carbon (C) and nitrogen (N) datasets from the whole-watershed fertilization experiment (1989–2018). (a) Map shows the locations of the principal study sites in the reference watershed (Ref WS7) and adjacent N-fertilized watershed (+N WS3). (b) Timeline indicates the years when data were collected (grey bars) and when C and N content were measured on ecosystem components (star). The plot in (b) was created using BIOPENDER (<https://biorender.com/>).

of the experiment (Helvey & Kunkle, 1986) and about quadruple the rate of N deposition at the end of the experiment (NADP site WV18; CASTNET site PAR107). Fertilizer treatments were distributed in three unequal applications per yr that roughly mimicked the temporal pattern of ambient deposition. An adjacent watershed (Ref WS7; 24 ha) serves as a reference to the fertilized watershed (Adams *et al.*, 2006). Forest stands in the watersheds were *c.* 18–19 yr old when the experiment began (1989; Table 1). Differences in land use history are summarized in Table 1, with a major difference being that Ref WS7 was maintained barren with herbicides for 3–6 yr before recovery, which likely contributed to the greater baseline streamwater nitrate (NO_3^-) flux before treatment (Fig. S5; see also Kochenderfer & Wendel, 1983; Kochenderfer, 2006). Tree species are similar in both watersheds; however, their relative abundance differs slightly, with +N WS3 dominated by *Prunus serotina* Ehrh. and *Acer rubrum* L. and Ref WS7 dominated by *Liriodendron tulipifera* L., *P. serotina* and *Betula lenta* L. (Fig. S1). One N-fixing tree, *Robinia pseudoacacia* L., is present in both watersheds and, according to tree censuses in 2016 and 2018, makes up < 7% of the basal area in the Ref WS7 and < 1% in +N WS3.

Assessing the impacts of N additions on watershed C and N budgets

In this study, we synthesized a variety of data collected by several researchers over the course of the experiment to construct

watershed-level C and N budgets, to gain insight into the response of biogeochemical cycles to chronic N additions and to assess the implications for the temperate forest C sink. These data were collected over various time scales and locations (Fig. 1), and the budgets provided an integrated picture of the C and N stocks after > 25 yr of N additions (typically from data collected between 2012–2019). In this section we describe the methods used to determine major C and N pools (e.g. aboveground biomass, fine root biomass, and soil stocks) and fluxes (e.g. aboveground net primary productivity (ANPP), foliar N resorption, fine root production, soil respiration, and inorganic N discharge). The budgets were also used to examine how N additions influence plant resource economics (e.g. C partitioning and the C cost of N acquisition). The C and N concentrations of many ecosystem components were determined using standard methods, especially Dumas combustion using an elemental analyzer (e.g. NA 1500 Series 2; Carlo Erba Instruments, Milan, Italy). When combining datasets across various years or plots, standard errors were propagated analytically (Methods S1; Lehrter & Cebrian, 2010). Additional details on data collection are found in the Supporting Information (Table S3; Methods S1–S4).

Aboveground biomass and productivity

Aboveground woody biomass was estimated from permanent growth plot data collected by the USFS Northern Research Station (Fig. 1; Adams *et al.*, 2006). Briefly, all trees > 2.54 cm in

diameter at breast height (DBH) were measured and permanently tagged at 25 randomly located 405-m² plots established in 1990 (+N WS3) or 1991 (Ref WS7). All trees were re-measured during the dormant seasons of 1996, 1999, 2003, 2009, and the summer of 2018. Diameter at breast height was converted to biomass increments using species-specific allometric equations (Brenneman *et al.*, 1978; M. B. Adams, unpublished data). For species without specific allometric parameters, we used parameters from tree species with similar wood densities (Miles & Smith, 2009).

To estimate total aboveground woody C and N pools, wood C and N concentrations were applied to the 2018 growth-plot biomass estimates. Wood C and N concentrations of the outer 1 cm of bole wood were measured in the summer of 2016 from 10 trees of each of the four dominant tree species in both watersheds (Table S1). Because wood N concentrations are often greater in the outer 1 cm of bole wood, we multiplied N content by a heartwood : sapwood ratio of 0.76 to obtain conservative estimates of wood N stocks (Meerts, 2003). For unsampled tree species, the watershed average wood C and N concentrations were used.

Mean annual rates of net aboveground wood C and N accumulation were calculated using the difference between pools of two consecutive DBH censuses (growth + ingrowth – mortality) divided by the number of yr between measurements. To estimate total ANPP, annual leaf litterfall mass data (1989–2015, $n = 25$) were converted into C flux estimates and added to net wood C increments (see Adams, 2008). Neither species composition nor nutrient concentrations of the long-term litterfall data were measured, so the C and N inputs of fine litter were estimated from 10 additional litter-collection plots in the autumns of 2015–2017 (Fig. 1; Methods S2; Table S2). Assuming litter mass varied more from year to year than litter C concentrations, we applied the mean of all plot-level litter C concentrations (total g of C per g of leaf litter) across 3 yr ($n = 30$) to the long-term litterfall mass data ($n = 25$). Total ANPP was estimated for each plot and then averaged to determine the mean watershed ANPP ($n = 25$), and standard error was propagated analytically (Methods S1).

Fine root pools, production, and turnover

Methods of fine root measurements are detailed in Table S3. Briefly, fine root biomass was measured in the organic horizon in the summers of 2012, 2013 and 2015. In 2012 and 2013, two subsamples of fine roots in the organic horizon were measured at seven plots (Fig. 1; W. T. Peterjohn, unpublished data); in 2015, one organic horizon sample was collected from the same plots plus three additional plots per watershed (see Carrara *et al.*, 2018). Fine root biomass was measured in the mineral horizon in 1991, 2013, 2015 and 2016 to depths of 45, 15, 15 and 10 cm, respectively (Adams, 2016; W. T. Peterjohn, unpublished data; Carrara *et al.*, 2018; B. A. Eastman & W. T. Peterjohn, unpublished data). In 2016, fine roots in the mineral soil (10 cm) were measured at 60 locations (six subsamples \times 10 plots) per watershed. Fine roots collected in 2012, 2013 and 2016 were analyzed for C and N concentration. To compare fine root C and N stocks

between years, the mean C and N concentrations of fine roots measured in 2012, 2013 and 2016 were applied to 1991 and 2015 fine root biomass. To adjust for the shallower depth of sampling in 2016 (0–10 cm vs 0–15 cm), the 2016 mass estimates were increased 150% when performing statistical analysis across years.

Fine root production and turnover were measured for two 1-year periods from 2016 to 2018 in the top 10 cm of mineral soil using cylindrical, 2-mm mesh, in-growth cores filled with homogenized, root-free, mineral soil (B. A. Eastman & W. T. Peterjohn, unpublished data). Four in-growth cores were deployed in 10 plots for 1 yr, after which cores were removed, soil and roots were collected, and new mineral soil was put into the cores for the second yr. Fine roots (< 2 mm) were hand-picked, rinsed with deionized water, and dried at 65°C for > 48 h before mass determination. Fine root turnover was estimated from the annual rates of root ingrowth measured in 2016–2018 divided by the root biomass stock measured in 2016. Fine root C and N concentrations from 2016 were applied to biomass production and turnover.

Annual N uptake and foliar N resorption

To examine how chronic N additions impacted the N acquisition strategies of trees, we estimated N uptake and its components. For this study, N uptake is defined as the total flux of soil N to fine roots and aboveground plant tissues, minus foliar N resorption, which simplifies to:

$$N_{\text{uptake}} = N_{\text{wood}} + N_{\text{litter}} + N_{\text{froot}} \quad \text{Eqn 1}$$

where N_{wood} is the N content of the annual increment of aboveground woody biomass (2009–2018); N_{litter} is the annual amount of N returned to the soil in leaf litter (2015–2017), which assumes resorption from green leaves to litter is in steady state; and N_{froot} is the amount of N associated with annual fine root N production (0–10 cm; 2016–2018). We calculated N uptake for each watershed using mean watershed values of wood, litter and fine root production, and standard error was propagated analytically (Methods S1).

Nitrogen concentrations of canopy leaves were measured in July 2012 on three leaves from each of four dominant tree species in 10 plots (Methods S3). In July 2016, an additional 8–11 trees of another species (*Quercus rubra*) were sampled for foliar N concentration, and watershed means from these data were combined with the 2012 data. For species not selected for foliar N analysis (< 15% of total leaf litter mass) we randomly sampled from the grand mean and standard deviation of N concentrations for each watershed. Foliage mass was estimated from plot-level leaf litter mass (from 2016 to 2018). We accounted for mass loss during senescence by multiplying litter mass by 1.27, the mean temperate deciduous ratio of green to senesced leaf mass (Van Heerwaarden *et al.*, 2003). This correction avoids large bias in underestimating foliar resorption and resorption efficiency. To estimate the total foliar N pool (N_{foliage}), mean N concentrations by species were multiplied by corrected foliage mass by species at the plot level, and then averaged for each watershed.

Nitrogen retranslocation ($N_{\text{foliage}} - N_{\text{litter}}$) and N resorption efficiency ($(N_{\text{foliage}} - N_{\text{litter}}) / N_{\text{foliage}}$) were estimated at the plot level, using data from the years available (foliage in 2012 and 2016, and litter in 2015–2017).

Soil C and N stocks

In 2016, soil C and N concentrations were measured at 15 soil pits (30.5×30.5 cm; Fig. 1) per watershed. Soil samples were collected from the organic horizon and 0–10, 10–20, 20–30, and 30–45 cm depths of the mineral soil. Samples were sieved to 2 mm, air-dried in a glasshouse, and ground before C and N analysis. Fine earth bulk density (coarse fragment-free; g m^{-3}) was measured for the 0–5 cm depth of mineral soil at 100 locations per watershed in 2011 (Gilliam *et al.*, 2018), and for the 15–45-cm depth at three quantitative soil pits at a nearby site in the Fernow (Adams *et al.*, 2004). These measured bulk densities were regressed on soil depth to calculate values for each depth at which C and N concentrations were measured (Fig. S2). To account for differences in the volume of coarse fragments between watersheds, we corrected the fine earth bulk density estimates for coarse fragment volume by horizon as measured in both watersheds ($n = 25$; Adams, 2016). Specifically, fine earth bulk densities of each soil depth were corrected using the mean proportion of coarse fragments of the corresponding soil horizon. Total C and N stocks for mineral soils were calculated for each depth increment as the product of soil C or N concentrations, depth increment, and corrected bulk density.

The mean mass of the organic horizon (g m^{-2}) was estimated from two (25×25 cm) measurements at seven plots in June of 2012 and 2013 (Fig. 1). For both watersheds, C and N concentrations of the organic horizon measured in 2016 ($n = 15$) were multiplied by the mean organic horizon mass per area measured in 2012 and 2013 to estimate the total C and N stocks. Error in these estimates represents plot-to-plot variability in both the C and N concentrations and organic horizon mass.

Soil and stream C and N fluxes

Total belowground C flux (TBCF) consists of the C flux to fine root production and maintenance, mycorrhizal associations, and root exudates often directed to the acquisition of N (Hobbie, 2006; Hobbie & Hobbie, 2008; Högberg *et al.*, 2010). We estimated TBCF at 10 plots per watershed (Fig. 1) using a mass balance approach (Raich & Nadelhoffer, 1989):

$$\text{TBCF} = R_s - \text{leaf litter C} \quad \text{Eqn 2}$$

where annual C inputs from leaf litter (2015) were subtracted from annual soil CO_2 efflux (R_s), assuming that the annual change in the soil C pool and soil C leaching losses were negligible (Giardina & Ryan, 2002). In 2016–2017, soil respiration, temperature, and moisture were measured weekly during the growing season and biweekly–monthly during the winter in the same plots where litterfall-C was collected (Fig. 1; Methods S4). Annual soil CO_2 efflux was estimated from an Arrhenius model

of soil respiration vs soil temperature (van't Hoff, 1898; Lloyd & Taylor, 1994), applied to data from hourly soil temperature measurements from the same plots (Methods S4).

Carbon losses through leaching were difficult to estimate due to a lack of measurements, although intermittent measurements of dissolved organic C (DOC) concentrations in streamwater are available from 2007 (W. T. Peterjohn, unpublished data; Edwards & Wood, 2011). Streamwater DOC concentrations were measured 12 times in +N WS3 and eight times in Ref WS7 in March–November of 2007, and a rough estimate of DOC discharge was obtained by multiplying the mean of all concentrations for each watershed by the annual stream discharge of water.

Soil N inputs from leaf litterfall were measured in 10 plots per watershed in 2015 and 2016 along with litter C inputs, as described in 'aboveground biomass and productivity' section. Nitrogen inputs from wet and dry atmospheric deposition were measured at NADP and CASTNET sites WV18 and PAR107. The +N WS3 also received $3.5 \text{ g N m}^{-2} \text{ yr}^{-1}$ from experimental fertilizations of $(\text{NH}_4)_2\text{SO}_4$ (Table 1).

Nitrogen losses in stream water were estimated from continuous streamflow measurements and streamwater chemistry sampled weekly or biweekly since 1983 by the USFS Northern Research Station near weirs at the base of each watershed (Edwards & Wood, 2011). Volume-weighted monthly means of streamwater NO_3^- and NH_4^+ concentrations from January 1984 through December 2017 were multiplied by the corresponding total monthly streamwater discharge to calculate export rates from each watershed. Monthly N export values were summed to arrive at annual estimates of dissolved inorganic N discharge. Because we lack consistent measurements of particulate or dissolved organic N in streamwater, we were unable to estimate dissolved organic N export.

We did not include gaseous N losses in our budget, and from the few measurements of production rates and emissions of N-containing trace gases (NO and N_2O) in these watersheds (Peterjohn *et al.*, 1996; Venterea *et al.*, 2004), it seems unlikely that their combined flux would exceed $c. 0.1 \text{ g N m}^{-2} \text{ yr}^{-1}$. However, gaseous N losses are difficult to measure, and unmeasured N_2 losses could account for a portion of budget imbalances.

C partitioning and C cost of N acquisition

To determine whether trees shift their C partitioning to favor aboveground vs belowground C flux under chronic N additions, we compared C fluxes to ANPP vs TBCF. We also estimated the C cost of soil N acquisition (N_{acq}) for each watershed using a previously published formula (Fisher *et al.*, 2010; Brzostek *et al.*, 2014; Shi *et al.*, 2019):

$$\text{C cost of N}_{\text{acq}} (\text{g C g N}^{-1}) = \frac{(\text{TBCF} (\text{g C m}^{(-2)} \text{ yr}^{(-1)}))}{(\text{N}_{\text{acq}} (\text{g N m}^{(-2)} \text{ yr}^{(-1)}))} \quad \text{Eqn 3}$$

Although TBCF can be expended for other purposes (e.g. uptake of other resources, and protection from aluminum toxicity), N is typically the most limiting nutrient in forests of this

region. Thus, our calculations assume this TBCF is directed for N acquisition, and these estimates may be conservatively considered an upper estimate for the C cost of Nacq.

Statistical analysis

To control for initial differences in aboveground C stocks, an analysis of covariance (ANCOVA) tested for watershed differences in biomass C, using 1991 estimates of basal area as an independent covariate. As wood N stock estimates did not differ between watersheds in the early years, a one-way analysis of variance (ANOVA) was used to test for watershed differences in wood N stocks in recent years. To control for initial conditions and to account for repeated measures, watershed differences in C production in woody biomass and aboveground NPP were assessed with a repeated measures mixed effects ANOVA where watershed (WS), year, and WS \times year were fixed effects, 1991 basal area was a covariate, and plot was a random effect. Foliar N pools and N retranslocation were compared between watersheds using a mixed-effects ANOVA with watershed as the main effect and year as a random effect. A one-way ANOVA also tested watershed differences in soil C and N pools, which had only one observation per plot ($n = 15$), and reported error represents plot-to-plot spatial variability. Watershed differences in litterfall C and N production (2015–2017) were tested using a nested ANOVA, with watershed as a fixed effect and year as a random nested effect within watershed. Similarly, watershed differences in fine root biomass and soil respiration were tested using a nested ANOVA, with watershed as a fixed effect, year as a random nested effect within watershed, and plot as a random nested effect within watershed.

As is common in watershed-scale and other large ecosystem experiments, this study is an example of simple pseudoreplication, as each watershed represents an experimental treatment with a sample size of one (Hurlbert, 1984). Results should be

interpreted with this in mind, but given the duration and extent of the treatment, differences found are most likely treatment effects rather than characteristic differences between watersheds.

Residuals of all ANOVA models were tested for normality (Shapiro–Wilk test), and where this assumption was not met, observations were transformed to meet ANOVA assumptions. When reported, back-transformed means \pm standard errors are identified in figures and tables. Most statistical analyses were executed in R v.3.6.1 (R Core Team, 2019) using the LME4 package for mixed-effects ANOVAs (Bates *et al.*, 2015), and least square means were calculated using the LSMEANS package (Lenth & R., 2016). Nested ANOVA models were performed in SAS JMP (JMP, v.14; https://www.jmp.com/en_us/home.html).

Results

Aboveground biomass and productivity

As expected for an aggrading forest, aboveground woody biomass increased during the experiment in both the fertilized and unfertilized watersheds, though at a faster rate in +N WS3 (Fig. 2a; $F = 8.607$, $P = 0.005$, $n = 25$). Autumnal leaf litterfall mass did not differ between watersheds and increased at the same rate in both watersheds since 1991 (*c.* 12 g yr⁻¹; $P_{year} < 0.001$; Fig. 2b). From nutrient analyses of 2015 and 2016 leaf litter (Table S2), we estimated a slightly greater return of litter C and N and a lower C : N ratio for leaf litter in +N WS3 (Table 2; $F = 32.37$, $P < 0.001$, $n = 10$). Controlling for the greater basal area in +N WS3 at the beginning of the study, repeated measures ANOVA found that ANPP (g C m⁻² yr⁻¹) was *c.* 25% greater in +N WS3 over the course of the study (Fig. 2c; Table 2; $F = 13.63$, $P < 0.001$, $n = 25$). Furthermore, the C : N ratio of woody biomass in the +N WS3 was *c.* 35% greater (Table 2; $F = 103$, $P < 0.001$, $n = 25$).

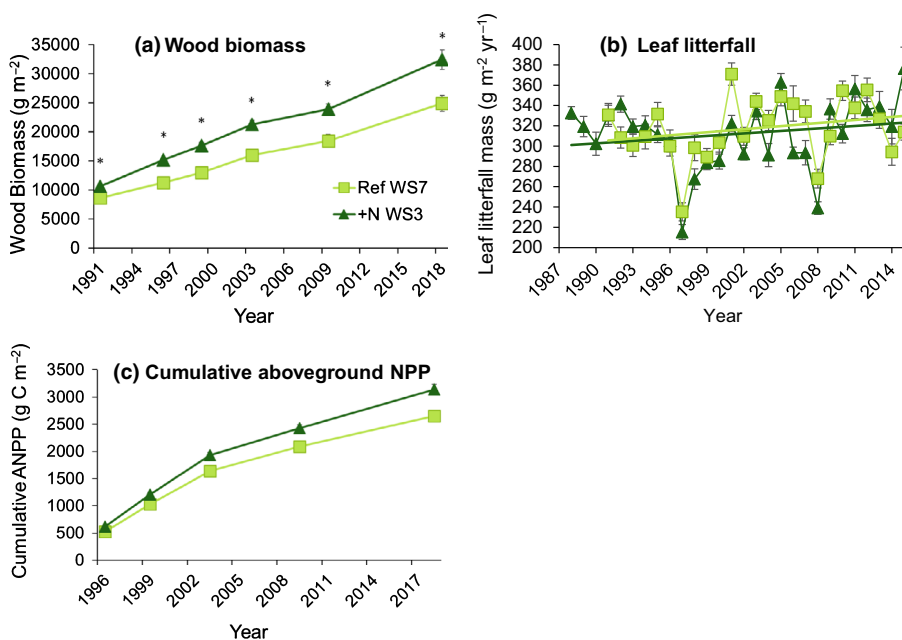


Fig. 2 Long-term data on aboveground biomass productivity showed greater rates of (a) woody biomass stock increase (growth + ingrowth – mortality), (b) equal leaf litterfall production, and (c) greater cumulative aboveground net primary productivity (ANPP) carbon (C) in the fertilized watershed. Points are mean values from 25 plots per watershed in the fertilized watershed (+N WS3, dark green triangles) and the reference watershed (Ref WS7, light green squares). Error bars represent ± 1 SE. Trend lines in (b) litterfall production fit by linear regression, and slopes do not differ between watersheds.

Belowground biomass and productivity

Fine root biomass varied among years: organic horizon fine root C stocks were greater in +N WS3 in two of the three years measured and lower in one (Fig. S3), and mineral fine root C stocks trended lower in +N WS3 in 1991, 2013 and 2015 but trended greater when measured to 10-cm depth in 2016 (Fig. S3). Fine root N stocks followed the same pattern as the C stocks, and the C : N ratios of fine root pools did not differ between watersheds (Table 2). However, when patterns in biomass were considered collectively with their tissue concentrations, fine root C and N stocks from 2012–2016 were smaller in the organic horizon of +N WS3 ($P_C = 0.011$, $P_N = 0.002$, $n = 18$), and not detectably different in the upper mineral horizon (0–15 cm; Table 2). Fine root pools of C and N in the upper mineral soil did not change significantly over time. Furthermore, fine root production and turnover (0–10 cm depth) did not differ between watersheds (Table 2).

Annual N uptake and foliar N resorption

Nitrogen pools of green canopy leaves were unexpectedly lower in +N WS3 (Table 2; $F = 4.57$, $P = 0.037$, $n = 10$). Because

foliar N concentrations did not differ between watersheds when comparing single species (Table S4), this distinction in foliar N pools is likely driven by slight differences in species composition, where low foliar N species (*A. rubrum* and *Q. rubra*) are more abundant in +N WS3, and one particularly high foliar N species (*L. tulipifera*) is more abundant in Ref WS7 (Fig. S1; Table S4). This distinction may be conservative since it does not account for the greater abundance of *R. pseudoacacia* (a high N-content, N-fixing species) in Ref WS7 (Fig. S1). Alternatively, leaf litter mass in the 10 litter chemistry plots (Fig. 1a) was slightly lower in +N WS3 for the three years used to estimate foliar mass (2015–2017), despite the lack of long-term differences in litter mass. Even so, foliar N retranslocation was 22% less, by mass, in the +N WS3 (Table 2; $F = 14.46$, $P = 0.001$, $n = 10$), and the N resorption efficiency was also lower in +N WS3 (Table 2; $F = 24.93$, $P < 0.001$, $n = 10$). Despite less N retranslocation in +N WS3, soil N uptake was similar in both watersheds (Table 2).

Soil C and N stocks

No differences in organic horizon C pools, N pools, or C : N ratios were detected between watersheds (Fig. 3). Despite

Table 2 Carbon and nitrogen budgets for reference watershed (Ref WS7) and the adjacent N-fertilized watershed (+N WS3).

Ecosystem component	Year	Carbon†		Nitrogen†		C : N ratio	
		Ref WS7	+N WS 3	Ref WS7	+N WS3	Ref WS7	+N WS3
Pools							
Woody biomass (g m ⁻²)	2018	11,475 (634) *	15,364 (801)	28 (6)	29 (8)	416 (10) ***	560 (6.4)
Foliage (g m ⁻²)	2012–2016	262 (49)	228 (42)	12.0 (1.7) *	10.0 (1.4)	21.9 (0.2)	22.3 (0.3)
Fine root biomass (g m ⁻²)	2012–2016						
OH		31 (3.5) *	18 (2.5)	1.08 (0.09) **	0.65 (0.12)	29.4 (2.6)	28.0 (2.3)
Mineral (0–15 cm)		121 (32)	110 (30)	3.6 (0.8)	3.1 (0.7)	28.6 (1.0)	29.4 (0.8)
Soil (OH-45 cm; g m ⁻²)	2016	8838 (513)‡	9801 (1,055)‡	638 (40)‡	656 (59)‡	13.8 (1.2)	14.9 (2.1)
Total ecosystem pool (g m ⁻²)		20 465 (816)	25 293 (1,325)	671 (40)	689 (60)		
Fluxes							
Wood production (g m ⁻² yr ⁻¹)	2009–2018	400 (24) ***	545 (42)	1.01 (0.06)	0.97 (0.07)	406 (8) ***	556 (13)
Wood mortality (g m ⁻² yr ⁻¹)	2009–2018	98 (10)	69 (21)	0.14 (0.11)	0.18 (0.19)		
Leaf litter input (g m ⁻² yr ⁻¹)	2009–2018	162 (2)	156 (3)	3.8 (0.05)	4.3 (0.08)	43 (1.7) ***	37 (1.8)
ANPP (g C m ⁻² yr ⁻¹)	2009–2018	565 (25) ***	709 (43)	–	–	–	–
N uptake (g N m ⁻² yr ⁻¹) ^a	2009–2018	–	–	7.6 (2.4)	8.7 (2.0)	–	–
Foliar N retranslocation (g m ⁻² yr ⁻¹)	2016	–	–	8.2 (1.7) **	6.0 (1.4)	–	–
N resorption efficiency (%)	2016	–	–	67.8 (9.7) ***	60.5 (9.8)	–	–
Fine root production (0–10 cm; g m ⁻² yr ⁻¹) ^b	2016–2018	89 (9)	122 (9)	2.8 (0.2)	3.4 (0.2)	41.0 (1.4)	42.8 (1.0)
Fine root turnover (0–10 cm; yr ⁻¹) ^c	2016–2018	0.92 (0.1)	1.03 (0.1)	0.63 (0.07)	0.62 (0.06)	–	–
Respiration (g C m ⁻² yr ⁻¹) ^d	2016–2017	982 (63) *	864 (28)	–	–	–	–
TBCF (g C m ⁻² yr ⁻¹) ^d	2016–2017	838 (67) *	724 (29)	–	–	–	–
Stream export (g m ⁻² yr ⁻¹) ^e	2009–2018	83	73	1.08 (0.06) **	1.68 (0.09)	–	–
C cost of N uptake (g C g ⁻¹ N) ^f		110 (12)	83.5 (6.7)				

Asterisks represent statistical difference between watersheds (*, $P = 0.05$; **, $P < 0.01$, ***, $P < 0.001$). † Means of pools and fluxes (standard error).

‡ Denotes back-transformed means (maximum SE) of log_e-transformed data.

^aN acquired from soil: N uptake = N wood increment + N leaf litter + N fine root production_(0–10 cm).

^bFrom B. A. Eastman *et al.* (unpublished).

^cFrom B. A. Eastman *et al.* (unpublished), estimated by dividing mean fine root production (over 2 yr) from initial fine root biomass measured before inserting in-growth cores.

^dFrom B. A. Eastman *et al.* (unpublished). TBCF = fine litterfall inputs minus soil CO₂-C efflux.

^eC leaching losses from 2007 are from intermittent streamwater dissolved organic C concentration measurements.

^fC cost of N uptake = TBCF/N-uptake from watershed means, with standard errors propagated analytically.

measuring mineral soil C and N at 15 locations per watershed, statistical comparisons between watersheds were strongly affected by the high spatial variability of mineral soil C (CV = 15–67%) and N (CV = 48–76%), and no differences between watersheds were found between total soil C or N pools to a depth of 45 cm. However, we did find that C pools were 1328 g C m^{-2} larger, and N pools were 84 g N m^{-2} larger in the surface (0–10 cm) mineral soil of the +N WS3 at $\alpha = 0.1$ (Fig. 3; $F_C = 3.588$, $P_C = 0.069$; $F_N = 4.206$, $P_N = 0.050$; $n = 15$), consistent with more numerous observations of the 0–5 cm soil increment ($n = 100$, $P < 0.05$; Gilliam *et al.*, 2018). The C : N ratio of soil was significantly higher for all depth increments in +N WS3, with the exception of the 0–10 cm increment (Fig. 3; $F_{10-10\text{cm}} = 5.353$, $P_{10-20\text{cm}} = 0.028$; $F_{20-30\text{cm}} = 4.81$, $P_{20-30\text{cm}} = 0.037$; $F_{30-45\text{cm}} = 4.688$, $P_{30-45\text{cm}} = 0.039$; $n = 15$). However, the C : N ratio of the 0–5 cm of mineral soil, when measured at 100 locations per watershed, exhibited a greater C : N ratio (17.6 in +N WS3 vs 14.6 in Ref WS7; see Gilliam *et al.*, 2018; $F = 4.04$, $P < 0.001$, $n = 100$), underscoring the benefits of a larger sample size when characterizing highly heterogeneous ecosystem stocks.

Soil and stream C and N fluxes

Measured rates of soil respiration and estimated values for the annual soil $\text{CO}_2\text{-C}$ efflux were *c.* 14% lower in +N WS3 from June 2016–May 2018, despite similar soil temperatures in both watersheds and greater soil moisture in the +N WS3 (Fig. S4; B. A. Eastman & W. T. Peterjohn, unpublished data). Because aboveground litter inputs and fine root production were both similar between the watersheds, this reduced

output (soil respiration) in +N WS3 drove the *c.* 12% lower TBCF (Table 2).

Based on infrequent measurements of streamwater dissolved organic C (DOC) in 2007, we estimated that +N WS3 had 12% lower C loss in streamwater DOC than Ref WS7 (Table 2). While quite uncertain, these estimates suggest that the export of DOC in streamflow may account for over 10% of total C losses from the ecosystem, and better measurements would be useful for a more complete picture of TBCF and biogeochemistry at this site.

As expected, stream-water inorganic N losses were much greater in +N WS3, representing more than one-third of total N inputs to that watershed. Cumulative N inputs (ambient + experimental) in +N WS3 were five times greater than N inputs to Ref WS7, or *c.* 100 g N m^{-2} greater (Table 1). However, cumulative N exports from 1989–2018 in +N WS3 exceeded Ref WS7 exports by only 12 g N m^{-2} (Fig. 4). Over a 29-yr period during this study (1989–2018), the total apparent N retained in +N WS3 was 98 g N m^{-2} , leading to annual increases in the ecosystem N stock in the absence of significant gaseous N losses. From the N mass balance budgets, there was a large missing N sink in +N WS3 and a comparatively small but substantial (13 g N m^{-2}) missing N source in Ref WS7 (Figs 4, S5).

C partitioning and C cost of N acquisition

Nitrogen fertilization resulted in a shift in N acquisition strategy and C partitioning (Fig. 5a). In response to N additions, +N WS3 retranslocated less foliar N before senescence, acquiring a greater proportion of total N flux from the soil compared to Ref WS7 (Fig. 5b). Assuming TBCF represents the maximum C cost

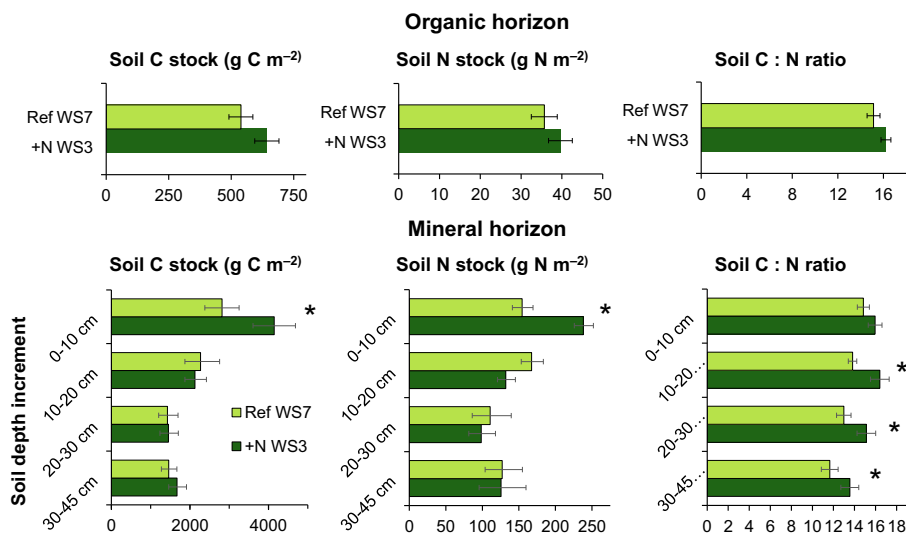


Fig. 3 Carbon (C) stocks (left), nitrogen (N) stocks (center), and C : N ratios (right) in the organic horizon (top) and surface mineral soil (bottom) of reference watershed 7 (light green) and fertilized watershed 3 (dark green). Results showed greater C and N stocks in surface mineral soil of +N WS3, and a greater C : N ratio of deeper mineral soil in +N WS3. Means ± 1 SE (error bars). All mineral soil and N stocks present back-transformed means of \log_e -transformed data except for the soil C 0–10 cm stock. Given the high spatial variability, the threshold for significant differences was $\alpha = 0.1$. Asterisks represent significant differences between watersheds (*, $P < 0.10$).

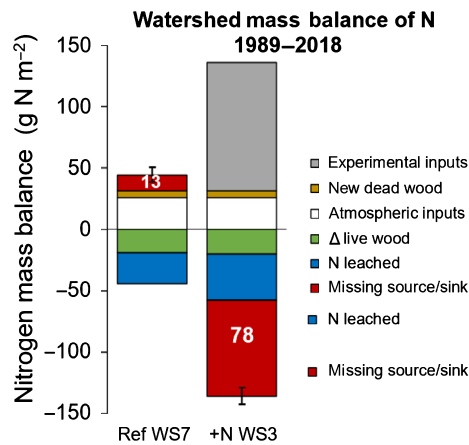


Fig. 4 Cumulative watershed nitrogen (N) budgets for reference watershed 7 (left) and fertilized watershed 3 (right) from 1989 to 2018. N inputs include experimental N additions (grey; 1989–2017 in +N WS3 only), atmospheric N deposition (white; 1989–2017), and wood N inputs from mortality (gold; 1990–2018). N outputs include live wood N accumulation (green; 1990–2018) and inorganic N losses in streamwater (blue; 1989–2017). Missing source/sink (red) is the difference between all N inputs and all N outputs. Error bars represent ± 1 SE, which was propagated analytically when summing the fluxes for which error terms existed (wood mortality and wood accumulation).

of N acquisition (Fisher *et al.*, 2010; Gill & Finzi, 2016; Terrer *et al.*, 2016), and considering TBCF was *c.* 14% less in +N WS3, we estimated that the maximum C cost of N uptake in +N WS3 ($83.2 \text{ g C g N}^{-1}$) was *c.* 27 g C g N^{-1} lower than in Ref

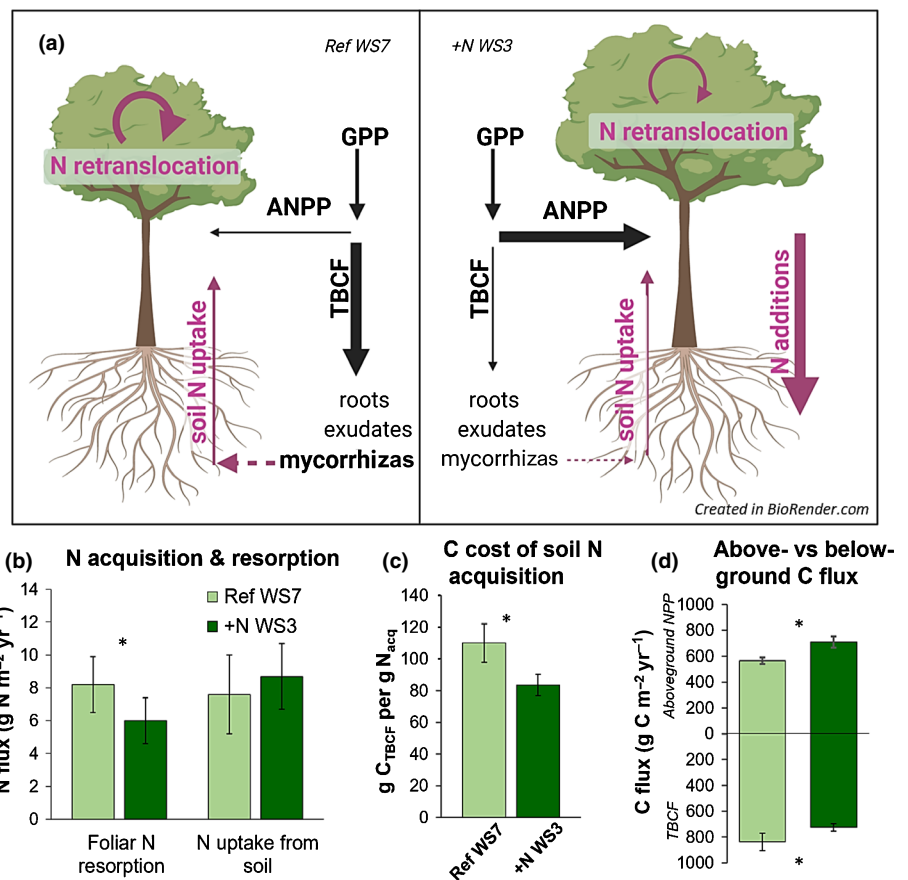
WS7 (110 g C g N^{-1} ; Fig. 5c). Thus, partitioning of photosynthate shifted away from belowground components and towards aboveground woody biomass production with N additions (Fig. 5).

Discussion

We synthesized a unique and diverse set of site-specific information to assess how > 25 yr of $(\text{NH}_4)_2\text{SO}_4$ additions altered C and N storage and partitioning at the Fernow Experimental Forest. Our findings indicate that generalizations from optimal allocation theory (Bloom *et al.*, 1985) can scale to an entire ecosystem through a shift in N acquisition strategy under enhanced N inputs. Specifically, we observed greater ecosystem C storage in aboveground woody biomass (Fig. 2a), less C transferred belowground (Fig 5d), and increased soil C storage and soil C : N ratios in the +N WS3 (Fig. 3). The shift in soil stoichiometry (greater C : N), as well as the increased proportion of plant biomass with high residence times (wood vs leaves and roots), may have long-term impacts on forest recovery in this ecosystem and other forests in the northeastern USA by potentially slowing N cycling (Craine *et al.*, 2018; Groffman *et al.*, 2018).

Increases in aboveground C storage dominated the ecosystem response to long-term N additions, as most of the *c.* 24% greater ecosystem C stock in +N WS3 was due to greater C flux to woody C (Table 2). This enhanced aboveground C accumulation

Fig. 5 Conceptual diagram of interactions between nitrogen (N) acquisition strategies and carbon (C) partitioning and corresponding mean fluxes of C and N. (a) Conceptual diagram of the interactions between C partitioning of gross primary productivity (GPP) to aboveground net primary productivity (ANPP) and total belowground C flux (TBCF) and N acquisition strategies between Ref WS7 (left) and +N WS3 (right). With greater soil N availability in +N WS3, less N is retranslocated from foliage and less C is partitioned belowground, allowing for greater partitioning of ANPP. (b) Mean (\pm SE) flux of N to meet N requirement from foliar N resorption and N uptake from soil in Ref WS7 (light green) and +N WS3 (dark green). (c) C cost of soil N acquisition (mean \pm SE) in the reference (light green) and fertilized (dark green) watersheds. C cost of soil N acquisition estimated by dividing TBCF by soil N uptake. N uptake = woody N accumulation + fine root N production – litter N flux. (d) C flux to ANPP and TBCF (mean \pm SE) for the reference (light green) and fertilized (dark green) watersheds. TBCF estimated with the mass balance equation: total soil respiration – leaf litter-C. Asterisks represent significant difference between watersheds (*, $P < 0.05$).



was noted in several meta-analyses of N addition experiments on seedlings and younger trees (Xia & Wan, 2008; Janssens *et al.*, 2010; Schulte-Uebbing & de Vries, 2017), but this study demonstrates that this pattern can persist in more mature forests (see also Pregitzer *et al.* 2008). Furthermore, we may have underestimated the N effect on biomass accumulation because Ibáñez *et al.* (2016) found that N fertilization widens the height : DBH ratio of some trees; this could create a potential bias when using standard allometric equations that do not include height (such as those used in this study) in fertilization experiments. Indeed, terrestrial LiDAR analysis conducted in 2016 found that trees in the +N WS3 were 2.4 m taller, on average, than those measured in WS7 (Atkins *et al.*, 2020). Although stand-level data (including in-growth and mortality) used in this study found a greater overall rate of biomass production with N additions (Fig. 2), this effect may diminish in the future. Recent tree-ring data for mature trees of several species document slower growth in the +N WS3 relative to Ref WS7 (Fig. S6; Malcomb *et al.*, 2020). Thus, the enhanced cumulative ANPP detected in +N WS3 may represent an initial positive response by fast-growing and acid-tolerant *P. serotina*, but this response may not persist due to a relative decline in tree growth among several dominant species (Fig. S6).

Under N limitation, a large proportion of assimilated plant C can be expended on N acquisition via mycorrhizas and foliar N resorption (Fahey *et al.*, 2005; Högborg *et al.*, 2010; Gill & Finzi, 2016). However, following N additions, more N can be acquired directly by roots through passive uptake, reducing the partitioning of C for N retranslocation, active transport, or mycorrhizal symbioses (Fig. 5a; Vitousek, 1982; Rastetter *et al.*, 2001; Fisher *et al.*, 2010; Brzostek *et al.*, 2014). Given similar foliar N pools and, thus, likely similar rates of GPP in these watersheds, our observation of less foliar N retranslocation (Table 2) and less mycorrhizal colonization (Carrara *et al.*, 2018) in +N WS3 suggest greater N uptake directly by roots. This 'cheaper' (in terms of C expenditure) strategy for N acquisition could free up C for woody biomass production (Fig. 5a; Holopainen & Peltonen, 2002; Wright & Westoby, 2003). While lower rates of N resorption from leaves in the +N WS3 suggest a lower N use efficiency (Fig. 5, Table 2), we still estimated a stimulation in C storage at the ecosystem scale (roots + soil + woody biomass) of *c.* 46 g C per g N experimentally added over the course of the experiment, which is in the range of values typically reported in other studies (30–75 g C g⁻¹ N; Hyvönen *et al.*, 2008; Pregitzer *et al.*, 2008; Sutton *et al.*, 2008). Given that the C cost of N acquisition in this study was *c.* 24% 'cheaper' in the fertilized watershed, the reduction in C flux belowground for N uptake in +N WS3 could account for over half of the enhanced ANPP (Table 2). This shift in C partitioning under N additions is consistent with theories and reviews of photosynthate allocation in plants (Litton *et al.*, 2007).

In addition to the greater woody C accumulation in the +N WS3, we detected a slightly greater C pool in the surface mineral soil of +N WS3 (0–10 cm; $a = 0.10$), despite similar inputs of fine plant litter. Interestingly, although N additions lowered the C : N ratio of leaf litter inputs (Tables 2, S2), the C : N ratio of

SOM is greater in +N WS3, suggesting that an important disconnect occurred in the soil environment between the stoichiometry of substrates (leaf litter) and products (SOM). This alteration of organic matter stoichiometry was found by other studies in temperate forests (Nave *et al.*, 2009; Yanai *et al.*, 2013; Forstner *et al.*, 2019). A possible explanation for this pattern is that reduced TBCF slowed the priming of organic matter decomposition by depriving soil microbes of labile C inputs from plants, allowing the accumulation of recalcitrant plant material with high C : N ratios in the surface soil (Kuzyakov, 2010; Cotrufo *et al.*, 2015; Sulman *et al.*, 2017). Though speculative, this proposed mechanism is supported by the reductions in soil respiration (Fig. S4) and mycorrhizal colonization (Carrara *et al.*, 2018) in the +N WS3. Furthermore, previous studies at this site measured slower leaf litter decomposition rates (Adams & Angradi, 1996) and lower ligninolytic enzyme activity in the +N WS3 – beyond what is expected from the reduced pH in +N WS3 (Carrara *et al.*, 2018; SanClements *et al.*, 2018). However, if the decay of any enhanced soil C stock in +N WS3 is inhibited by N additions, this C pool could become susceptible to decomposition and promote greater N availability once experimental N inputs subside. Alternatively, more N-limited trees in Ref WS7 may promote priming through increased TBCF to gain access to microbially mineralized N, and C losses associated with this priming could be greater than any reduced potential for SOC formation through TBCF in the +N WS3.

Given the potential for ecosystem-scale interactions that operate over decades to influence forest ecosystem responses to N additions, this study highlights the value of long-term, watershed-scale experiments in gaining insight into how above- and below-ground components interact and respond to environmental change. However, there are also limitations to the approach used in this – and other – watershed-scale studies due to a lack of replicated treatments. In the case of our study sites, causal attribution is confounded by differences in species composition (Fig. S1) and land use history (Table 1) that must be carefully considered when interpreting the results. However, the large dose of added N and subsequent changes in streamwater nutrient export and soil chemistry support our view that the +N WS3 is primarily responding to the treatment (Adams *et al.*, 2006). Furthermore, there is a nearby (< 2 km from our study sites), fully replicated, N-fertilization experiment with the same annual N additions as +N WS3 (Adams *et al.*, 2004). This replicated study has been used to test observations from the watershed experiment and confirm many of these responses – including enhanced tree productivity (Fowler *et al.*, 2015), reduced soil respiration (B. A. Eastman & W. T. Peterjohn, unpublished data), and lower mycorrhizal colonization and soil enzyme activity (Carrara *et al.*, 2018).

One invaluable feature of watershed-scale studies is the ability to create mass balance budgets at a broad spatial scale. From the watershed N budgets we constructed, over our 29-yr study period (1989–2018), the total apparent N retained in +N WS3 was 98 g N m⁻². The accumulation of N in vegetation N pools in both watersheds was slight (20 g N m⁻²), explaining only 20% of the N retention in +N WS3. Changes in soil stocks are very difficult to measure, even at decadal time scales, and the lack of

good pretreatment measurements and robust bulk density measurements in these watersheds prevents us from confidently estimating the change in the soil N stock over the experimental period. However, if the watershed differences in mean soil N stocks of the top 10 cm of mineral soil (84 g N m^{-2}) indicates a fertilization effect in the +N WS, this difference could account for the missing N sink in +N WS3 (Fig. 4). This would be consistent with other N fertilization studies that detected greater soil C and N stocks in the surface soil layers (Frey *et al.*, 2014; Pregitzer *et al.*, 2008; Zak *et al.*, 2008). Alternatively, unmeasured gaseous N losses and dissolved organic N outputs in streamwater could account for part of the imbalance (Enanga *et al.*, 2017). In Ref WS7, the missing source could be attributed to some combination of the following: N fixation by black locust (potentially $c. 1.89 \text{ g N m}^{-2}$; Fig. S7; free-living N fixation ($2.9\text{--}14.5 \text{ g N m}^{-2}$; Schlessinger & Bernhardt, 2020); errors in estimates of wood N – based on only the outer 1 cm of bole wood; or errors in estimates of gaseous N deposition.

Globally, the positive response of aboveground productivity to N additions appears to be strongest in temperate forests (Fleischer *et al.*, 2015; Du & de Vries, 2018), where N limitation may be the historical norm. Given that the positive growth responses of forests to increasing atmospheric CO_2 and longer growing seasons are often constrained by N availability and N acquisition strategies (Norby *et al.*, 2010; Fernández-Martínez *et al.*, 2014; Feng *et al.*, 2015; Smith *et al.*, 2016; Terrer *et al.*, 2019), a mechanistic representation of plant controls on soil–microbe interactions – and their subsequent feedbacks on soil nutrient cycling and plant productivity – are necessary for global C models to accurately predict the potential for forests to mitigate climate change through C sequestration (Wieder *et al.*, 2015, 2019; Sulman *et al.*, 2018, 2019; Shi *et al.*, 2019). This study provides a unique perspective on ecosystem-scale C responses to altered N inputs, and the importance of studying both above- and below-ground responses to environmental change. Future research focused on clarifying the mechanisms governing plant–soil interactions and quantifying the impact of N status on these processes may be critical, because it is uncertain whether this enhanced C storage will persist in the future – especially if ecosystem productivity becomes constrained over time due to changes in the patterns and processes of plant resource allocation that feedback on soil biogeochemistry.

Acknowledgements

We thank the staff at the USDA Forest Service, Northern Research Station, Parsons, WV, for their long-term support of research activities at the Fernow Experimental Forest and for supplemental data, especially Melissa Thomas-VanGundy, Pamela Edwards, Frederica Wood and Chris Cassidy. Thank you to the many undergraduate interns for tremendous assistance with field sampling and lab analysis, especially Hannah Minihan, Rachel McCoy, Zachary Sherman, Matt Green, Liz Matejczyk and Andrea Blankenship. Funding for this research and support for BAE and WTP were provided by the Long-Term Research in Environmental Biology (LTREB) program at the National Science Foundation (Grant nos. DEB-0417678 and DEB-

1019522). Funding to support JEC was provided by the National Science Foundation Graduate Research Fellowship under Grant no. DGE-1102689.

Author contributions

All authors collaborated on the conceptualization and manuscript outline facilitated by BAE, ERB and CK. All authors contributed to the writing of the manuscript, led by BAE. BAE analyzed the data and drafted all sections of the manuscript with key inputs from WTP and ERB. CAW contributed Fig. 1a and contributed to data analysis. BEM, MBA and MBB contributed foliar leaf chemistry datasets; MBB contributed wood chemistry datasets; JEC and ERB contributed fine root mass data; BAE, MBB and WTP contributed leaf litter chemistry datasets; BAE and WTP contributed soil respiration, TBCF, and fine root in-growth and turnover datasets.

ORCID

Edward R. Brzostek  <https://orcid.org/0000-0002-2964-0576>
 Mark B. Burnham  <https://orcid.org/0000-0002-0876-3606>
 Joseph E. Carrara  <https://orcid.org/0000-0003-0597-1175>
 Brooke A. Eastman  <https://orcid.org/0000-0003-3723-9616>
 Charlene Kelly  <https://orcid.org/0000-0001-5772-1405>
 Brenden E. McNeil  <https://orcid.org/0000-0002-2665-8383>
 Christopher A. Walter  <https://orcid.org/0000-0003-3264-2211>

References

- Adams MB. 2008. Long-term litterfall mass from three watersheds on the Fernow Experimental Forest, West Virginia. 16th Central Hardwoods Forest Conference, USDA Forest Service 304: 179–186.
- Adams MB. 2016. *Fernow experimental forest watershed acidification root data, 1991*. Parsons, WV, USA: Department of Agriculture, Forest Service, North Central Research Station.
- Adams MB, Angradi TR. 1996. Decomposition and nutrient dynamics of hardwood leaf litter in the Fernow Whole-Watershed Acidification Experiment. *Forest Ecology and Management* 83: 61–69.
- Adams MB, Burger J, Zelazny L, Baumgras J. 2004. *Description of the fork mountain long-term soil productivity study: site characterization*. Newtown Square, PA, USA: US Forest Service Northern Research Station.
- Adams MB, DeWalle DR, Hom JL eds. 2006. *The Fernow Watershed Acidification Study*. Dordrecht, the Netherlands: Springer.
- Adams MB, Edwards PJ, Ford WM, Schuler TM, Thomas-Van Gundy M, Wood F. 2012. *Fernow experimental forest: research history and opportunities*. Washington, DC, USA: USDA Forest Service.
- Atkins JW, Bond-Lamberty B, Fahey RT, Haber LT, Stuart-Haëntjens E, Hardman BS, LaRue E, McNeil BE, Orwig DA, Stovall AEL *et al.* 2020. Application of multidimensional structural characterization to detect and describe moderate forest disturbance. *Ecosphere* 11: e03156.
- Averill C, Waring B. 2017. Nitrogen limitation of decomposition and decay: how can it occur? *Global Change Biology* 24: 1417–1427.
- Bates D, Mächler M, Bolker B, Walker S. 2015. Fitting linear mixed-effects models using lme4. *Journal of Statistical Software* 67: 1–48.
- Bellassen V, Viovy N, Luyssaert S, le Maire G, Schelhaas M, Ciais P. 2011. Reconstruction and attribution of the carbon sink of European forests between 1950 and 2000. *Global Change Biology* 17: 3274–3292.
- Bloom AJ, Chapin FS, Mooney HA. 1985. Resource limitation in plants: an economic analogy. *Annual Review of Ecology and Systematics* 16: 363–392.

- Brenneman BB, Frederick DJ, Gardner WE, Schoenhofen LH, Marsh PL. 1978. Biomass of species and stands of West Virginia hardwoods. In *Proceedings of Central Hardwood Forest Conference II*. West Lafayette, IN, USA: Purdue University, 159–178.
- Brzostek ER, Fisher JB, Phillips RP. 2014. Modeling the carbon cost of plant nitrogen acquisition: mycorrhizal trade-offs and multipath resistance uptake improve predictions of retranslocation. *Journal of Geophysical Research: Biogeosciences* 119: 1684–1697.
- Carrara JE, Walter CA, Hawkins JS, Peterjohn WT, Averill C, Brzostek ER. 2018. Interactions among plants, bacteria, and fungi reduce extracellular enzyme activities under long-term N fertilization. *Global Change Biology* 24: 2721–2734.
- Chapman SK, Langley JA, Hart SC, Koch GW. 2006. Plants actively control nitrogen cycling: uncorking the microbial bottleneck. *New Phytologist* 169: 27–34.
- Cotrufo MF, Soong JL, Horton AJ, Campbell EE, Haddix ML, Wall DH, Parton WJ. 2015. Formation of soil organic matter via biochemical and physical pathways of litter mass loss. *Nature Geoscience* 8: 776–779.
- Craine JM, Elmore AJ, Wang L, Aranibar J, Bauters M, Boeckx P, Crowley BE, Dawes MA, Delzon S, Fajardo A *et al.* 2018. Isotopic evidence for oligotrophication of terrestrial ecosystems. *Nature Ecology and Evolution* 2: 1735–1744.
- Davies-Barnard T, Meyerholt J, Zaehle S, Friedlingstein P, Brovkin V, Fan Y, Fisher R, Jones C, Lee H, Peano D *et al.* 2020. Nitrogen cycling in CMIP6 land surface models: progress and limitations. *Biogeosciences* 17: 5129–5148.
- Drake JE, Gallet-Budynek A, Hofmockel KS, Bernhardt ES, Billings SA, Jackson RB, Johnsen KS, Lichter J, McCarthy HR, McCormack ML *et al.* 2011. Increases in the flux of carbon belowground stimulate nitrogen uptake and sustain the long-term enhancement of forest productivity under elevated CO₂. *Ecology Letters* 14: 349–357.
- Du E, de Vries W. 2018. Nitrogen-induced new net primary production and carbon sequestration in global forests. *Environmental Pollution* 242: 1476–1487.
- Edwards PJ, Wood F. 2011. *Fernow Experimental Forest daily streamflow*. Newtown Square, PA, USA: U.S. Department of Agriculture, Forest Service, Northern Research Station. Updated 09 January 2020. doi: 10.2737/RDS-2011-0015
- Enanga EM, Casson NJ, Fairweather TA, Creed IF. 2017. Nitrous oxide and dinitrogen: the missing flux in nitrogen budgets of forested catchments? *Environmental Science and Technology* 51: 6036–6043.
- Fahey TJ, Tierney GL, Fitzhugh RD, Wilson GF, Siccama TG. 2005. Soil respiration and soil carbon balance in a northern hardwood forest ecosystem. *Forestry* 35: 244–253.
- Feng Z, Rütting T, Pleijel H, Wallin G, Reich PB, Kammann CI, Newton PCD, Kobayashi K, Luo Y, Uddling J. 2015. Constraints to nitrogen acquisition of terrestrial plants under elevated CO₂. *Global Change Biology* 21: 3152–3168.
- Fernández-Martínez M, Vicca S, Janssens IA, Sardans J, Luysaert S, Campioli M, Chapin FS III, Ciais P, Malhi Y, Obersteiner M *et al.* 2014. Nutrient availability as the key regulator of global forest carbon balance. *Nature Climate Change* 4: 471–476.
- Fisher JB, Sitth S, Malhi Y, Fisher RA, Huntingford C, Tan S-Y. 2010. Carbon cost of plant nitrogen acquisition: a mechanistic, globally applicable model of plant nitrogen uptake, retranslocation, and fixation. *Global Biogeochemical Cycles* 24: GB003621.
- Fisher RA, Wieder WR, Sanderson BM, Koven CD, Oleson KW, Xu C, Fisher J, Shi M, Walker AP, Lawrence DM. 2019. Parametric controls on vegetation responses to biogeochemical forcing in the CLM5. *Journal of Advances in Modeling Earth Systems* 11: 2879–2895.
- Fleischer K, Wårlind D, Van Der Molen MK, Rebel KT, Arneth A, Erisman JW, Wassen MJ, Smith B, Gough CM, Margolis HA *et al.* 2015. Low historical nitrogen deposition effect on carbon sequestration in the boreal zone. *Journal of Geophysical Research: Biogeosciences* 120: 2542–2561.
- Forstner SJ, Wechselberger V, Müller S, Keibinger KM, Díaz-Piñés E, Wanek W, Scheppi P, Hagedorn F, Gundersen P, Tatzber M *et al.* 2019. Vertical redistribution of soil organic carbon pools after twenty years of nitrogen addition in two temperate coniferous forests. *Ecosystems* 22: 379–400.
- Fowler D, Coyle M, Skiba U, Sutton MA, Cape JN, Reis S, Sheppard LJ, Jenkins A, Grizzetti B, Galloway JN *et al.* 2013. The global nitrogen cycle in the twenty-first century. *Philosophical Transactions of the Royal Society of London. Series B: Biological Sciences* 368: 20130164.
- Fowler ZK, Adams MB, Peterjohn WT. 2015. Will more nitrogen enhance carbon storage in young forests stands in central Appalachia? *Forest Ecology and Management* 337: 144–152.
- Frey SD, Ollinger S, Nadelhoffer K, Bowden R, Brzostek E, Burton A, Caldwell BA, Crow S, Goodale CL, Grandy AS *et al.* 2014. Chronic nitrogen additions suppress decomposition and sequester soil carbon in temperate forests. *Biogeochemistry* 121: 305–316.
- Galloway JN, Trends R, Townsend AR, Erisman JW, Bekunda M, Cai Z, Freney JR, Martinelli LA, Seitzinger SP, Sutton MA. 2008. Transformation of the nitrogen cycle: potential solutions. *Science* 320: 889–892.
- Giardina CP, Ryan MG. 2002. Total belowground carbon allocation in a fast-growing eucalyptus plantation estimated using carbon balance approach. *Ecosystems* 5: 487–499.
- Gill AL, Finzi AC. 2016. Belowground carbon flux links biogeochemical cycles and resource-use efficiency at the global scale. *Ecology Letters* 19: 1419–1428.
- Gilliam FS, Walter CA, Adams MB, Peterjohn WT. 2018. Nitrogen (N) dynamics in the mineral soil of a Central Appalachian hardwood forest during a quarter century of whole-watershed N additions. *Ecosystems* 21: 1489–1504.
- Groffman PM, Driscoll CT, Durán J, Campbell JL, Christenson LM, Fahey TJ, Fisk MC, Fuss C, Likens GE, Lovett G *et al.* 2018. Nitrogen oligotrophication in northern hardwood forests. *Biogeochemistry* 141: 523–539.
- Helvey JD, Kunkle SH. 1986. *Input-output budgets of selected nutrients on an experimental watershed near Parsons*. WV. Res. Pap. NE-584. USDA Forest Service, Northeastern Experiment Station, Broomall, PA, USA.
- Hobbie EA. 2006. Carbon allocation to ectomycorrhizal fungi correlates with belowground allocation in culture studies. *Ecology* 87: 563–569.
- Hobbie EA, Hobbie JE. 2008. Natural abundance of ¹⁵N in nitrogen-limited forests and tundra can estimate nitrogen cycling through mycorrhizal fungi: a review. *Ecosystems* 11: 815–830.
- van't Hoff JH. 1898. Lectures on theoretical and physical chemistry. In: *Chemical dynamics Part I*. London, UK: Edward Arnold, 224–229.
- Högberg MN, Briones MJI, Keel SG, Metcalfe DB, Campbell C, Midwood AJ, Thornton B, Hurry V, Linder S, Näsholm T *et al.* 2010. Quantification of effects of season and nitrogen supply on tree below-ground carbon transfer to ectomycorrhizal fungi and other soil organisms in a boreal pine forest. *New Phytologist* 187: 485–493.
- Holopainen JK, Peltonen P. 2002. Bright autumn colours of deciduous trees attract aphids: nutrient retranslocation hypothesis. *Oikos* 99: 184–188.
- Hurlbert SH. 1984. Pseudoreplication and the design of ecological field experiments. *Ecological Monographs* 54: 187–211.
- Hyvönen R, Persson T, Andersson S, Olsson B, Ågren GI, Linder S. 2008. Impact of long-term nitrogen addition on carbon stocks in trees and soils in northern Europe. *Biogeochemistry* 89: 121–137.
- Ibáñez I, Zak DR, Burton AJ, Pregitzer KS. 2016. Chronic nitrogen deposition alters tree allometric relationships: implications for biomass production and carbon storage. *Ecological Applications* 26: 913–925.
- Ise T, Litton CM, Giardina CP, Ito A. 2010. Comparison of modeling approaches for carbon partitioning: impact on estimates of global net primary production and equilibrium biomass of woody vegetation from MODIS GPP. *Journal of Geophysical Research: Biogeosciences* 115: 1–11.
- Janssens IAA, Dieleman W, Luysaert S, Subke J, Reichstein M, Ceulemans R, Ciais P, Dolman AJ, Grace J, Matteucci G *et al.* 2010. Reduction of forest soil respiration in response to nitrogen deposition. *Nature Geoscience* 3: 315–322.
- Johnson NC, Graham JH, Smith FA. 1997. Functioning of mycorrhizal associations along the mutualism–parasitism continuum. *New Phytologist* 135: 575–585.
- Kochenderfer JN. 2006. Fernow and the appalachian hardwood region. In: Adams MB, DeWalle DR, Hom JL, eds. *the Fernow watershed acidification study*. Dordrecht, the Netherlands: Springer, 17–39.
- Kochenderfer JN, Wendel GW. 1983. Plant succession and hydrologic recovery on a deforested and herbicided watershed. *Forest Science* 29: 545–558.
- Kuzakov Y. 2010. Priming effects: interactions between living and dead organic matter. *Soil Biology and Biochemistry* 42: 1363–1371.

- LeBauer DS, Treseder KK. 2008. Nitrogen limitation of net primary productivity in terrestrial ecosystems is globally distributed. *Ecology* **89**: 371–379.
- Lehrter JC, Cebrian J. 2010. Uncertainty propagation in an ecosystem nutrient budget. *Ecological Applications* **20**: 508–524.
- Lenth RV. 2016. Least-squares means: the R package lsmeans. *Journal of Statistical Software* **69**: 1–33.
- Litton CM, Raich JW, Ryan MG. 2007. Carbon allocation in forest ecosystems. *Global Change Biology* **13**: 2089–2109.
- Liu L, Greaver TL. 2010. A global perspective on belowground carbon dynamics under nitrogen enrichment. *Ecology Letters* **13**: 819–828.
- Lloyd J, Taylor JA. 1994. On the temperature dependence of soil respiration. *Functional Ecology* **8**: 315–323.
- Lovett GM, Arthur MA, Weathers KC, Fitzhugh RD, Templer PH. 2013. Nitrogen addition increases carbon storage in soils, but not in trees, in an Eastern U.S. deciduous forest. *Ecosystems* **16**: 980–1001.
- Malcomb JD, Scanlon TM, Epstein HE, Druckenbrod DL, Vadeboncoeur MA, Lanning M, Adams MB, Wang L. 2020. Assessing temperate forest growth and climate sensitivity in response to a long-term whole-watershed acidification experiment. *Journal of Geophysical Research: Biogeosciences* **125**: 1–16.
- Meerts P. 2003. Mineral nutrient concentrations in sapwood and heartwood: a literature review. *Annals of Forest Science* **59**: 713–722.
- Meyerholt J, Sickel K, Zaehle S. 2020. Ensemble projections elucidate effects of uncertainty in terrestrial nitrogen limitation on future carbon uptake. *Global Change Biology* **26**: 3978–3996.
- Miles PD, Smith WB. 2009. *Specific gravity and other properties of wood and bark for 156 tree species found in North America*. Res. Note NRS-38. Newtown Square, PA, USA: US Department of Agriculture, Forest Service, Northern Research Station.
- Mohan JE, Cowden CC, Baas P, Dawadi A, Frankson PT, Helmick K, Hughes E, Khan S, Lang A, Machmuller M *et al.* 2014. Mycorrhizal fungi mediation of terrestrial ecosystem responses to global change. *Fungal Ecology* **10**: 3–19.
- Montané F, Fox AM, Arellano AF, MacBean N, Ross Alexander M, Dye A, Bishop DA, Trouet V, Babst F, Hessl AE *et al.* 2017. Evaluating the effect of alternative carbon allocation schemes in a land surface model (CLM4.5) on carbon fluxes, pools, and turnover in temperate forests. *Geoscientific Model Development* **10**: 3499–3517.
- Nave LE, Vance ED, Swanston CW, Curtis PS. 2009. Impacts of elevated N inputs on north temperate forest soil C storage, C/N, and net N-mineralization. *Geoderma* **153**: 231–240.
- Norby R, Warren J, Iversen C, Medlyn B, McMurtrie R. 2010. CO₂ enhancement of forest productivity constrained by limited nitrogen availability. *Proceedings of the National Academy of Sciences, USA* **107**: 19368–19373.
- O'Sullivan M, Spracklen DV, Batterman SA, Arnold SR, Gloor M, Buermann W. 2019. Have synergies between nitrogen deposition and atmospheric CO₂ driven the recent enhancement of the terrestrial carbon sink? *Global Biogeochemical Cycles* **33**: 163–180.
- Pan Y, Birdsey RA, Fang J, Houghton R, Kauppi PE, Kurz WA, Phillips OL, Shvidenko A, Lewis SL, Canadell JG *et al.* 2011. A large and persistent carbon sink in the world's forests. *Science* **333**: 988–993.
- Peterjohn WT, Adams MB, Gilliam FS. 1996. Symptoms of nitrogen saturation in two Central Appalachian hardwood forest ecosystems. *Biogeochemistry* **35**: 507–522.
- Phillips RP, Brzostek E, Midgley MG. 2013. The mycorrhizal-associated nutrient economy: a new framework for predicting carbon-nutrient couplings in temperate forests. *New Phytologist* **199**: 41–51.
- Pregitzer KS, Burton AJ, Zak DR, Talhelm AF. 2008. Simulated chronic nitrogen deposition increases carbon storage in Northern Temperate forests. *Global Change Biology* **14**: 142–153.
- Raich JW, Nadelhoffer KJ. 1989. Belowground carbon allocation in forest ecosystems: global trends. *Ecology* **70**: 1346–1354.
- Rastetter EB, Vitousek PM, Field CB, Shaver GR, Herbert D, Agren GI. 2001. Resource optimization and symbiotic nitrogen fixation. *Ecosystems* **4**: 369–388.
- R Core Team. 2020. *R: A language and environment for statistical computing*. Vienna, Austria: R Foundation for Statistical Computing. <https://www.R-project.org/>.
- SanClements MD, Fernandez IJ, Lee RH, Roberti JA, Adams MB, Rue GA, McKnight DM. 2018. Long-term experimental acidification drives watershed scale shift in dissolved organic matter composition and flux. *Environmental Science and Technology* **52**: 2649–2657.
- Schlesinger W, Burnhardt E. 2020. Biogeochemical cycling on land. In: *Biogeochemistry: an analysis of global change, 4th edn*. San Diego, CA, USA: Academic Press, 183–248.
- Schmidt MWI, Torn MS, Abiven S, Dittmar T, Guggenberger G, Janssens IA, Kleber M, Kögel-Knabner I, Lehmann J, Manning DAC *et al.* 2011. Persistence of soil organic matter as an ecosystem property. *Nature* **478**: 49–56.
- Schulte-Uebbing L, de Vries W. 2017. Global-scale impacts of nitrogen deposition on tree carbon sequestration in tropical, temperate, and boreal forests: a meta-analysis. *Global Change Biology* **24**: e416–e431.
- Shi M, Fisher JB, Brzostek ER, Phillips RP. 2016. Carbon cost of plant nitrogen acquisition: global carbon cycle impact from an improved plant nitrogen cycle in the Community Land Model. *Global Change Biology* **22**: 1299–1314.
- Shi M, Fisher JB, Phillips RP, Brzostek ER. 2019. Neglecting plant-microbe symbioses leads to underestimation of modeled climate impacts. *Biogeosciences* **16**: 457–465.
- Smith P, Davis SJ, Creutzig F, Fuss S, Minx J, Gabrielle B, Kato E, Jackson RB, Cowie A, Krieglner E *et al.* 2016. Biophysical and economic limits to negative CO₂ emissions. *Nature Climate Change* **6**: 42–50.
- Sulman BN, Brzostek ER, Medici C, Shevliakova E, Menge DNL, Phillips RP. 2017. Feedbacks between plant N demand and rhizosphere priming depend on type of mycorrhizal association. *Ecology Letters* **20**: 1043–1053.
- Sulman BN, Moore J, Abramoff R, Averill C, Kivlin S, Georgiou K, Sridhar B, Hartman M, Wang G, Wieder W *et al.* 2018. Multiple models and experiments underscore large uncertainty in soil carbon dynamics. *Biogeochemistry* **141**: 109–123.
- Sulman BN, Shevliakova E, Brzostek ER, Kivlin SN, Malyshev S, Menge DNL, Zhang X. 2019. Diverse mycorrhizal associations enhance terrestrial C storage in a global model. *Global Biogeochemical Cycles* **33**: 501–523.
- Sutton MA, Simpson D, Levy PE, Smith RI, Reis S, Van Oijen M, De Vries WIM. 2008. Uncertainties in the relationship between atmospheric nitrogen deposition and forest carbon sequestration. *Global Change Biology* **14**: 2057–2063.
- Terrer C, Jackson RB, Prentice IC, Keenan TF, Kaiser C, Vicca S, Fisher JB, Reich PB, Stocker BD, Hungate BA *et al.* 2019. Nitrogen and phosphorus constrain the CO₂ fertilization of global plant biomass. *Nature Climate Change* **9**: 684–689.
- Terrer C, Vicca S, Hungate BA, Phillips RP, Prentice IC. 2016. Mycorrhizal association as a primary control of the CO₂ fertilization effect. *Science* **353**: 72–74.
- Thornton PE, Lamarque JF, Rosenbloom NA, Mahowald NM. 2007. Influence of carbon-nitrogen cycle coupling on land model response to CO₂ fertilization and climate variability. *Global Biogeochemical Cycles* **21**: 1–15.
- Todd-Brown KEO, Randerson JT, Post WM, Hoffman FM, Tarnocai C, Schuur EAG, Allison SD. 2013. Causes of variation in soil carbon simulations from CMIP5 Earth system models and comparison with observations. *Biogeosciences* **10**: 1717–1736.
- Van Heerwaarden LM, Toet S, Aerts R. 2003. Current measures of nutrient resorption efficiency lead to a substantial underestimation of real resorption efficiency: facts and solutions. *Oikos* **101**: 664–669.
- Venterea RT, Groffman PM, Castro MS, Verchot LV, Fernandez IJ, Adams MB. 2004. Soil emissions of nitric oxide in two forest watersheds subject to elevated N inputs. *Forest Ecology and Management* **196**: 335–349.
- Vitousek PM. 1982. Nutrient cycling and nutrient use efficiency. *American Naturalist* **119**: 553–572.
- de Vries W, Du E, Butterbach-Bahl K. 2014. Short and long-term impacts of nitrogen deposition on carbon sequestration by forest ecosystems. *Current Opinion in Environmental Sustainability* **9**: 90–104.
- Wieder WR, Cleveland CC, Smith WK, Todd-Brown K. 2015. Future productivity and carbon storage limited by terrestrial nutrient availability. *Nature Geoscience* **8**: 441–444.
- Wieder WR, Lawrence DM, Fisher RA, Bonan GB, Cheng SJ, Goodale CL, Grandy AS, Koven CD, Lombardozzi DL, Oleson KW *et al.* 2019. Beyond

static benchmarking: using experimental manipulations to evaluate land model assumptions. *Global Biogeochemical Cycles* **33**: 1289–1309.

Wright IJ, Westoby M. 2003. Nutrient concentration, resorption and lifespan: leaf traits of Australian sclerophyll species. *Functional Ecology* **17**: 10–19.

Xia J, Wan S. 2008. Global response patterns of terrestrial plant species to nitrogen addition. *New Phytologist* **179**: 428–439.

Yanai RD, Vadeboncoeur MA, Hamburg SP, Arthur MA, Fuss CB, Groffman PM, Siccama TG, Driscoll CT. 2013. From missing source to missing sink: long-term changes in the nitrogen budget of a northern hardwood forest. *Environmental Science and Technology* **47**: 11440–11448.

Young D, Zégre N, Edwards P, Fernandez R. 2019. Assessing streamflow sensitivity of forested headwater catchments to disturbance and climate change in the central Appalachian Mountains region, USA. *Science of the Total Environment* **694**: 133382.

Zak DR, Freedman ZB, Upchurch R, Steffens M, Kögel-Knabner I. 2017. Anthropogenic N deposition increases soil organic matter accumulation without altering its biochemical composition. *Global Change Biology* **23**: 933–944.

Zak DR, Holmes WE, Burton AJ, Pregitzer KS, Talhelm AF. 2008. Simulated atmospheric NO_3^- deposition increases soil organic matter by slowing decomposition. *Ecological Applications* **18**: 2016–2027.

Supporting Information

Additional Supporting Information may be found online in the Supporting Information section at the end of the article.

Fig. S1 Mean percent basal area of eight dominant species in the reference and fertilized watersheds.

Fig. S2 Fine earth bulk density measurements and estimates.

Fig. S3 Mean fine root carbon (C) stocks in the organic horizon and surface mineral soil across 5 yr of measurements.

Fig. S4 Time series of soil respiration, temperature, and moisture data from 2016 to 2017 at the Fernow Watershed Fertilization study.

Fig. S5 Hydrologic inorganic N budgets for reference watershed 7 and fertilized watershed 3 over 34 calendar yr.

Fig. S6 Relationship of basal area increment of four dominant species between the reference and fertilized watersheds during pretreatment; and predicted basal area increments for the fertilized watershed, based on pretreatment relationship to the reference watershed.

Fig. S7 Mean black locust (*Robinia pseudoacacia*) stem density and annual estimated N fixation.

Methods S1 Methods for propagating error when combining datasets across various years or plots.

Methods S2 Materials and methods for leaf litter mass and chemistry analysis.

Methods S3 Materials and methods for green foliage collection and chemical analysis.

Methods S4 Soil respiration measurements and annual CO_2 efflux estimates.

Table S1 Mean (\pm SE) tree wood carbon and nitrogen concentrations for four tree species.

Table S2 Mean (\pm SE) leaf litter carbon and nitrogen concentrations, C : N ratios, and mass for five tree species.

Table S3 Methods for fine root measurements at the Fernow Experimental Forest Watershed Fertilization Experiment.

Table S4 Mean (\pm SE) green foliage carbon and nitrogen concentrations and C : N ratios for five tree species.

Please note: Wiley Blackwell are not responsible for the content or functionality of any Supporting Information supplied by the authors. Any queries (other than missing material) should be directed to the *New Phytologist* Central Office.